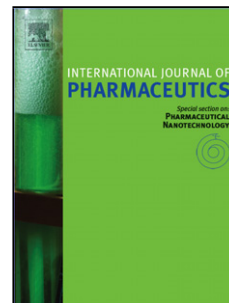


Accepted Manuscript

Title: Comparison of spray drying, electroblowing and electrospinning for preparation of Eudragit E and itraconazole solid dispersions

Author: Péter Lajos Sóti Katalin Bocz Hajnalka Pataki
Zsuzsanna Eke Attila Farkas Geert Verreck Éva Kiss Pál
Fekete Tamás Vigh István Wagner Zsombor K. Nagy György
Marosi



PII: S0378-5173(15)30094-6
DOI: <http://dx.doi.org/doi:10.1016/j.ijpharm.2015.07.076>
Reference: IJP 15080

To appear in: *International Journal of Pharmaceutics*

Received date: 11-5-2015
Revised date: 27-7-2015
Accepted date: 29-7-2015

Please cite this article as: Sóti, Péter Lajos, Bocz, Katalin, Pataki, Hajnalka, Eke, Zsuzsanna, Farkas, Attila, Verreck, Geert, Kiss, Éva, Fekete, Pál, Vigh, Tamás, Wagner, István, Nagy, Zsombor K., Marosi, György, Comparison of spray drying, electroblowing and electrospinning for preparation of Eudragit E and itraconazole solid dispersions. *International Journal of Pharmaceutics* <http://dx.doi.org/10.1016/j.ijpharm.2015.07.076>

This is a PDF file of an unedited manuscript that has been accepted for publication. As a service to our customers we are providing this early version of the manuscript. The manuscript will undergo copyediting, typesetting, and review of the resulting proof before it is published in its final form. Please note that during the production process errors may be discovered which could affect the content, and all legal disclaimers that apply to the journal pertain.

**Comparison of spray drying, electroblowing and electrospinning for preparation of
Eudragit E and itraconazole solid dispersions**

Péter Lajos Sóti^a, Katalin Bocz^a, Hajnalka Pataki^a, Zsuzsanna Eke^b, Attila Farkas^a, Geert Verreck^c, Éva Kiss^d, Pál Fekete^{a,e}, Tamás Vigh^a, István Wagner^a, Zsombor K. Nagy^a, György Marosi^{a*}

^a Department of Organic Chemistry and Technology, Budapest University of Technology and Economics, H-1111 Budapest, Műegyetem rkp. 3-9, Hungary

^b Joint Research and Training Laboratory on Separation Techniques, Eötvös Loránd University, H-1117 Budapest, Pázmány Péter sétány 1/a, Hungary

^c Janssen Research & Development, Beerse, Belgium

^d Institute of Chemistry, Eötvös Loránd University, H-1117 Budapest, Pázmány Péter sétány 1/a, Hungary

^e Meditop Pharmaceutical Ltd., H-2097 Pilisborosjenő, Ady Endre utca 1, Hungary

* Corresponding author at: Department of Organic Chemistry and Technology, Budapest University of Technology and Economics, Műegyetem rkp. 3-9, H-1111 Budapest, Hungary. Tel.: +36 1 463 3654; fax: +36 1 463 3648. E-mail address: gmarosi@mail.bme.hu (G. Marosi).

Graphical abstract

Abstract

Three solvent based methods: spray drying (SD), electrospinning (ES) and air-assisted electrospinning (electroblowing; EB) were used to prepare solid dispersions of itraconazole and Eudragit E. Samples with the same API/polymer ratios were prepared in order to make the three technologies comparable. The structure and morphology of solid dispersions were identified by scanning electron microscopy and solid phase analytical methods such as, X-ray powder diffraction (XRPD), differential scanning calorimetry (DSC) and Raman chemical mapping. Moreover, the residual organic solvents of the solid products were determined by static headspace-gas chromatography/mass spectroscopy measurements and the wettability of samples was characterized by contact angle measurement. The pharmaceutical performance of the three dispersion type, evaluated by dissolution tests, proved to be very similar. According to XRPD and DSC analyses, made after the production, all the solid dispersions were free of any API crystal clusters but about 10 wt% drug crystallinity was observed after three months of storage in the case of the SD samples in contrast to the samples produced by ES and EB in which the polymer matrix preserved the API in amorphous state.

Keywords: electrospinning, electroblowing, spray drying, Raman mapping, rapid dissolution, itraconazole

1. Introduction

Most of the active pharmaceutical ingredients (APIs) are commercialized in tablets or capsules (Anselmo and Mitragotri, 2014), which are most accepted by patients. Development of cost-efficient technologies for these solid forms of human and animal pharmaceuticals is of great importance.

The solubility of recently discovered APIs is often very poor (Macarron, 2006; Vasconcelos et al., 2007) in the gastrointestinal fluids, resulting in low oral bioavailability (Wong et al., 2006). Methods that are available to eliminate the solubility problem (Fahr and Liu, 2007; Sarode et al., 2014) are either costly or their industrial applicability is limited .

The dissolution rate of APIs belonging to, the BCS II group can effectively be improved by use of salt forms with enhanced dissolution profiles (Agharkar et al., 1976), by solubilisation of drugs in co-solvents (Amin et al., 2004), by micellar solutions (Torchilin, 2007), by formation of water-soluble complexes (Casella et al., 1998), by use of lipidic systems for the delivery of lipophilic drugs (Humberstone and Charman, 1997), by increasing the specific surface area of the API according to the Noyes–Whitney equation (Kawabata et al., 2011; Whitney and Noyes, 1897) or by forming solid dispersions of amorphous APIs (Sekiguchi et al., 1964; Simonelli et al., 1969; van Drooge et al., 2006). The combinations of the last two mentioned methods can be achieved by solvent based technologies, such as spray drying (SD) and electrospinning (ES).

Although SD is widely used in pharmaceutical technology for preparing micro- and/or nanoparticles (Asker and Becker, 1966; Draheim et al., 2015; Fontana et al., 2014), it has some disadvantages. SD technologies are energy consuming, heat-sensitive APIs can be decomposed during the drying process, and furthermore, the separation and handling of the produced fine powder can cause difficulties (Broadhead et al., 1992; Cal and Sollohub, 2010).

ES is a facile and straightforward process for creating polymeric nanofibres, which can be exploited as carriers for developing a series of new drug delivery systems (DDS) (Ignatious et al., 2010; Kenawy et al., 2002; Nagy et al., 2010; Vigh et al., 2013; Yu et al., 2013). Using ES processes, not only the above-mentioned disadvantages can be eliminated, but also some new types of solid dispersions can be developed for poorly water-soluble drugs, such as third generation solid dispersions and structural solid dispersions (Yu et al., 2011, 2010). As for the scale-up of ES, recent efforts such as a high speed electrospinning (HSES) have shown the promising future (Nagy et al., 2015).

Electroblowing (EB) is another scalable version of ES (Kim et al., 2003; Zhou et al., 2009) but the use of this technology for producing DDS is still under development (Balogh et al., 2015).

In this study, our aim was to compare the three solvent based technologies and their applicability for preparing Eudragit E based DDS containing itraconazole (ITR) as a model binary solid dispersion.

ITR is a well-known broad-spectrum antifungal agent (Glasmacher and Prentice, 2006) belonging to BCS II (Wu and Benet, 2005), the solid dispersions of which have been published with Eudragit E matrix by several authors (Janssens et al., 2010; Jung et al., 1999; Six et al., 2003). In these works, the miscibility limit and phase separation of amorphous and crystalline ITR were investigated in melt extruded polymer systems in comparison with film casting and SD. The experimental miscibility limit (15% w/w when prepared by film casting or 27.5% w/w prepared by SD below the T_g of the polymer) was found to be strongly dependent on the manufacturing technology and higher value were achieved than expected based on theoretical study (7.07% w/w) (Janssens et al., 2010). Stability tests were not included in these experimental programs.

Our aim was to examine further details of the mentioned critical characteristics (phase separation and the influence of the solvent evaporation rate) of ITR-Eudragit E systems after producing their solid dispersions by methods and to investigate their stability after a three month-storage by several methods.

2. Materials and methods

2.1. Materials

Crystalline ITR (with a purity of more than 99%) was obtained from Janssen Pharmaceutica (Beerse, Belgium). Eudragit® E was obtained from Evonik Industries (Darmstadt, Germany). Methanol, dichloromethane and concentrated HCl solution (it was diluted by purified water for dissolution media) were purchased from Merck Ltd. (Budapest, Hungary).

2.2. Preparation methods

ITR and Eudragit E were dissolved in a dichloromethane : methanol (4:1) solvent mixture and the resulting clear solutions were used for the preparation of solid samples. Spray-drying was performed with a Pro-Cep-T 4M8-TriX spray dryer (ProCept, Belgium). An infusion pump (Aitecs SEP-10S Plus syringe pump, Lithuania), a direct current power supplier (NT-35 High Voltage DC Supply MA2000, Hungary) and spinnerets (in case of the ES a single fluid nozzle, while in the case of EB bi-fluids nozzle) were used to perform electrospinning and electroblowing. The process parameters are summarized in Table 1. The solid dispersions were stored for three months (90 days) at room temperature at 30% RH to examine their stability.

2.3. Scanning electron microscopy (SEM)

The size and fine texture of the microparticles and fibres were investigated by a JEOL JSM 6380LA (Tokyo, Japan) scanning electron microscope (acceleration voltage: 10 – 30 kV). Each specimen was fixed with conductive double-sided carbon adhesive tape and sputtered with gold – palladium alloy (using a JEOL 1200 instrument) in order to render it electrically conductive.

2.4. Residual solvent measurement

The amount of residual solvent in the samples was determined using a static headspace-gas chromatography-mass spectrometry (HS-GC/MS) method. A 20 – 100 mg sample was weighed into a 10 mL vial and 1.50 g of anhydrous sodium sulfate and 3 mL of distilled water were added before crimping. The sample was thermostated for 20 minutes at 80 °C and agitated at 600 rpm. A 0.5 mL sample was collected from the headspace with a 2.5 mL headspace syringe which was thermostated at 105 °C. The sample was injected to a split/splitless injector in split injection mode at a 20:1 split ratio. Injector temperature was set at 180 °C. An Agilent 7890 gas chromatograph was used with a RTX-VMS (20 m × 180 μm × 1 μm) column and separation was carried out isothermally at 40 °C with a constant 1 mL/min flow of helium 5.0. The temperature of the transfer line, ion source and quadrupole were set at 250 °C, 230 °C, and 150 °C, respectively. The Agilent 5975C inert XL mass spectrometer was used in selected ion monitoring (SIM) mode with two SIM groups. Target ions were 29 (methanol) and 84 (dichloromethane); qualifier ions were 31 and 86, respectively; dwell time was 50 ms for each ions. External standard calibration was used. The stock solution for methanol was made with distilled water, for dichloromethane with

methanol, so two series of calibration solutions were prepared and measured. The calibration ranges were 20 – 1000 µg for methanol, and 0.3 – 100 µg for dichloromethane.

2.5. X-ray powder diffraction (XRPD) measurement

The pure itraconazole, Eudragit E and ITR-loaded microspheres and fibres were analysed with a PANalytical X'pert Pro X-ray MPD diffractometer (Almelo, The Netherlands). The measurements were under $\text{CuK}\alpha$ ($\lambda=1.5406 \text{ \AA}$), 40 kV and 30 mA as X-ray source with $\text{K}\beta$ (Ni) filter. The diffraction patterns were collected with 2θ ranging from 4° to 42° or 44° .

2.6. Differential scanning calorimetry (DSC) measurement and initial crystallinity determination

Thermal analyses of solid dispersions were carried out using TA Instruments Q2000 apparatus (New Castle, Delaware) in nitrogen atmosphere. The heating rate was $10^\circ\text{C}/\text{min}$, heating scans were performed from 25 to 200°C , and TA Instruments Universal Analysis 2000 software was used for data analysis. The determination of the degree of crystallization before the DSC treatment needed special attention as the 20% or 40% API ratio of the samples started to crystallize during heating in the DSC apparatus. Therefore, the “initial crystallinity of the drug” (Six et al., 2002) was used for comparison, which means the sum of the integrals of the exothermic crystallization and endothermic melting peaks. When the API in a sample was amorphous, the sum was below the detection level ($<3\%$). For the determination of initial crystallinity, the DSC curves were integrated from 110.0 to 175.0°C (ranges of crystallization and melting for ITR), the resulted heat of fusion (ΔH) was corrected with the API concentration in the solid dispersions, and it was compared with the fusion enthalpy of pure crystalline ITR. Purified indium standard was used to calibrate the instrument.

2.7. Raman mapping

Chemical mapping was carried out on electrospun, electroblown and spray-dried samples using LabRAM 300 micro-Raman spectrometer, manufactured by Horiba Jobin–Yvon (Longjumeau, France) equipped with an external diode laser source (785 nm, 400 mW) and an air cooled CCD detector. The spectra were recorded in the spectral range of 400-1835 cm^{-1} and the high resolution maps were collected with an objective of $\times 100$ magnification (laser spot size: $\sim 0.7 \mu\text{m}$) and 1 μm step size. The acquired image consisted of 41×41 points (pixels), each spectrum was acquired for 10 s, and 2 spectra were averaged in each pixel. For the visualization of the API distribution in the polymer matrix, piece-wise linear base-line correction was applied on all spectra (using the same baseline points for all the maps points and the reference spectra). Afterwards, spectra were normalized to unit area and the component concentrations were estimated with the classical least squares (CLSs) method using the reference spectra of the pure polymer and amorphous ITR. LabSpec 5.41.15 software was used for the spectral analyses and the visualization of chemical maps.

2.8. Dissolution test

In vitro drug dissolution tests were performed in 900 mL of 0.1 M HCl solution thermostated at $37 \pm 1 \text{ }^\circ\text{C}$ by means of a Pharma Test PTWS600 dissolution tester equipped with fully automated sampling system (Pharma Test, Hainburg, Germany), using the rotating basket apparatus (USP I) with 100 min^{-1} stirring speed. Previously ground fibrous samples and spray-dried microparticles containing 50 mg of the API were filled in the basket and the API concentration of the dissolution medium was determined by UV/VIS spectrophotometry (Hewlett-Packard - HP 8453 Diode Array UV/VIS spectrophotometer) at 254 nm based on a calibration line of standards with known concentration.

2.9. Contact angle measurements

The wettability of SD, ES and EB samples was characterized by means of a contact angle goniometer (Dataphysics OCA15+; Germany) using the static sessile drop method. 5 μL of 0.1 M HCl solution was dropped onto the surface of tablets compressed from the various samples (ITR preserved its amorphous form in the compressed tablets according to XRPD and DSC analyses.) at room temperature. An optical subsystem was used to capture the drop profile on tablets surface at 0 s and images were analysed using the ellipse fitting method following interface determination.

3. Results and discussion

3.1. Comparison of yields, productivity, morphology, and residual solvents

The composition of solid dispersions, yields, content uniformity and productivity are summarized in table 2. The yields of solid products could be increased in all cases by increasing ITR concentration. The yield of SD, owing to the handling of the fine powder product, was somewhat less, but it is noted that it can be overcome in case of continuous high-volume production. The deviation in the yields of the electrospun solid dispersions were in connection with the collection efficiency of the fibrous product. The same is true for the electroblown products. The productivity of ES could be improved effectively from 2 g/h to 56.7 g/h (see table 2) by the use of an assisting airflow. Thus, ~28 times higher productivity could be achieved than by using the single fluid nozzle. The content uniformity of the samples was checked by UV/VIS spectrometry after dissolving accurately measured samples in ethanol. The data suggest that the API content of solid dispersions correspond to the theoretical values in all cases with high content uniformity.

The products prepared by the three (ES, EB and SD) continuous evaporation processes can be seen in figure 1. In terms of fibre-morphology, the electrospun samples were bead-free fibrous mats with diameters between 0.2 and 5 μm (figure 1a and b). The texture of the EB dispersion was also fibrous, but some beaded fibres with low diameter range were detected in case of the EB_20 (see figure 1c and d) owing probably to the reduced concentration of the solid materials in the solution. The SEM images of the SD samples show spherical products in the diameter range of 1 to 30 μm (figure 1e and f).

The solvent evaporation methods applied to prepare solid dispersions are critical in respect of the residual organic solvent content, which has to be limited to an acceptably low level. Therefore, the residual organic solvents of the solid dispersions were determined by HS/GC-MS. The results are summarized in table 3.

Considering the European Medicines Agency's Guideline for Residual Solvents, these solid dispersions are fully compliant with the requirements. Residual methanol was below the calibration range in all the products, while the residual dichloromethane in the spray-dried sample (SD_40) was slightly beyond the lower limit of the calibration range, indicating a slight difference in the drying efficiency of the evaporation methods.

3.2. Comparison of the solid dispersions by XRPD, DSC and Raman mapping

XRPD analyses provided information about the physical state of ITR. The physical mixture at consisting of 20% w/w ITR and 80% polymer served as a reference (figure 2A g). The diffraction patterns suggest that ITR turned into amorphous form during all of the compared DDS-forming processes (see figure 2).

For getting further information about the state of ITR in these systems, the samples were examined by DSC as well. Four different exothermic and endothermic peaks appeared in the DSC curves of the crystallizable solid dispersions (figure 3, the DSC curve of SD_40 is characteristic of the transitions of all 40% w/w ITR loaded samples). The first peak belongs to the glass temperature (T_g) of the polymer and ITR, which includes the relaxation of the polymer matrix. The second endothermic signal at 89 °C corresponds to the transition from the chiral nematic mesophase to the isotropic liquid of ITR (Mt). The broad exothermic peak from 110 °C to 155 °C corresponds to the cold crystallization of ITR, which follows the melting of the drug crystals at 169 °C (Six et al., 2002).

The thermograms of the ES_20 and EB_20 samples did not show any peaks excepting the one caused by relaxation at the T_g transition (see table 4 and figure 4). The spray-dried sample (SD_20), which was amorphous according to the XRPD measurement (figure 2A e), shows exothermic and endothermic transition in its DSC curve suggesting some phase separation of amorphous matrix and amorphous drug, allowing cold crystallization and melting of ITR induced by heating.

Van den Mooter *et al.* also observed the influence of drying kinetics on the phase structure.

Raman microscopy can indicate specific interactions between components and determine their distribution in solid dispersions; therefore, such analyses were performed too. The Raman spectra of the ES, EB and SD samples could be very well approximated with the linear combinations of the reference spectra suggesting the absence of specific interactions between the ITR and polymer molecules, in accordance with earlier FT-IR results (Janssens et al., 2010). Clear evidence of phase separation was expected from the results of Raman mapping experiments. These maps are shown in figure 5.

The electrospun and electroblown samples (figure 5a, b, d, and e) did not show any inhomogeneity, while the spray-dried dispersions (figure 5c and f) were not perfectly homogeneous. The mixing level of polymer and ITR molecules remained high when electrostatic field was applied during the drying process. It corresponds to our recently published results (Sóti et al., 2015). The quantitative DSC data (table 4), in accordance with the XRPD diffraction patterns (figure 2), confirm that the samples were free of any crystal clusters after production.

The three-month storage of solid dispersions did not cause a characteristic change in the diffraction patterns: the XRPD measurements repeated after 90 days still did not show crystalline phase in the solid dispersions above the detection limit of the method (figure 2). However, differences could be detected by the DSC analysis of spray dried samples within the range of 110 and 175 °C (table 4). The degree of initial crystallinity of dispersions determined according to DSC measurements showed about 10 wt% ITR crystalline part in both SD_20 and SD_40, while the ES and EB products preserved the amorphous state of ITR (see table 4 and figure 2).

Considering the results of the solid phase analyses and the theoretical miscibility limit (cited in the introduction), the thermodynamically favoured phase separation of supersaturated solid dispersions was observed when the drying was proceed, in the case of spray drying, above the T_g of polymer, which facilitates the recrystallization of ITR. In turn, the ES and EB samples, which were prepared at room temperature and resulted in a homogenous distribution of ITR in the polymer matrix, had no tendency to crystallize at the storage conditions. (When the API/matrix ratio was raised from 1:4 to 2:3, the appearance of the mesophase transition and cold crystallization in DSC suggested some phase separation even for the ES and EB samples, but it happened only at submicronic level according to the homogeneous Raman maps.).

3.3. Dissolution results

The pharmaceutical performance of the dispersions was evaluated by measuring their dissolution properties in 0.1 M HCl (figure 6). The dissolution tests were performed for comparison on the physical mixtures of the crystalline drug and the polymer. The dissolution was 100% in the case of each solid dispersion sample after 40 min, which is a dramatic increase compared to the physical mixture, which can be ascribed to the fine solid dispersion of the mostly amorphous drug in the highly soluble tertiary amine type carrier. Moreover, by decreasing the API/matrix ratio (from 2:3 to 1:4) the total dissolution time of ITR could be reduced from 40 to 10 min. Based on the results, all the three solvent-based technologies are similarly applicable for improving the dissolution rate of ITR. The phase separation of the matrix and ITR, shown by DSC and Raman results, had no effect on the dissolution profile. During the applied storage period the solid dispersions preserved the improved dissolution rate and we observed no changes in the drug release. Even the spray dried dispersions behaved the same way in spite of their partial recrystallization according to DSC. In fact only the amorphous state is maintained even after the phase separation during the process, as detected by the Raman mapping, and only longer storage or DSC heat treatment induced the recrystallization.

For the interpretation of the observed differences between the dissolution profiles of the samples with different ITR content, the wettability of the samples was characterized by contact angle measurements. It was observed that the contact angles of the samples containing 40% w/w ITR are significantly higher than those of the 20% w/w ITR contained samples. The results in figure 7 are given for EB samples, which were the same for ES and SD within the margin of error. When the ITR concentration was increased in the dispersions, the DDS became more hydrophobic, thereby reducing the wettability of samples, which caused a somewhat slower drug release.

4. Conclusions

In this study, the electrospinning, electroblowing (air-assisted electrospinning) and spray-drying methods were compared for preparing itraconazol and Eudragit E solid dispersions. The productivity of ES could be improved effectively by the use of assisted airflow without any significant change in the drug dissolution profile, physical state and distribution of the API in the polymer matrix at all of the applied API/matrix ratios. The dissolution rate of ITR could be enhanced significantly compared to the physical mixtures of raw materials by all of the studied solvent evaporation methods. Although the XRPD analyses did not show any differences between the products of various drying processes, DSC and Raman mapping suggested phase separation of amorphous polymer and amorphous API in the case of the spray dried samples providing chance for recrystallization during the applied three-month storage period. The samples preserved the improved dissolution rate of ITR during the storage period in spite of partial segregation in the samples containing 40% ITR, and just started crystallization of the spray dried solid dispersions. The results indicated differences in the distribution of amorphous API in the supersaturated matrix leading to different probabilities of crystallization during storage. It highlights the importance of solvent evaporation rate when kinetically stable (but thermodynamically unstable) solid dispersions are prepared. These results point out also the capability of high resolution Raman mapping to determine subtle differences in the structure of amorphous solid dispersions (ASD) and indicate how the properties of ASD depend on the manufacturing and processing conditions. The 28-fold higher productivity of the electroblowing process compared to the related electrospinning method is promising for further improvement. By multiplying the spinnerets, the total output can be further increased. The pharmaceutical performance of EB product proved to be equivalent with the ES counterpart.

Acknowledgements

The research was supported by the OTKA Research Fund (code 112644 and code 108975). Besides this project is supported by the New Széchenyi Plan (Project ID: TÁMOP-4.2.1/B-09/1/KMR-2010-0002), János Bolyai Research Scholarship of the Hungarian Academy of Sciences and MedInProt project. The authors would like to express their gratitude to Dr. János Madarász (Budapest University of Technology and Economics, Hungary) for making XRPD measurements possible in his laboratory.

References

- Agharkar, S., Lindenbaum, S., Higuchi, T., 1976. Enhancement of solubility of drug salts by hydrophilic counterions: Properties of organic salts of an antimalarial drug. *J. Pharm. Sci.* 65, 747–749. doi:10.1002/jps.2600650533
- Amin, K., Dannenfelser, R.-M., Zielinski, J., Wang, B., 2004. Lyophilization of polyethylene glycol mixtures. *J. Pharm. Sci.* 93, 2244–2249. doi:10.1002/jps.20135
- Anselmo, A.C., Mitragotri, S., 2014. An overview of clinical and commercial impact of drug delivery systems. *J. Control. Release* 190, 15–28. doi:10.1016/j.jconrel.2014.03.053
- Asker, A.F., Becker, C.H., 1966. Some Spray-Dried Formulations of Sulfaethylthiadiazole for Prolonged-Release Medication. *J. Pharm. Sci.* 55, 90–94. doi:10.1002/jps.2600550119
- Balogh, A., Horváthová, T., Fülöp, Z., Loftsson, T., Harasztos, A.H., Marosi, G., Nagy, Z.K., 2015. Electroblowing and electrospinning of fibrous diclofenac sodium-cyclodextrin complex-based reconstitution injection. *J. Drug Deliv. Sci. Technol.* 26, 28–34. doi:10.1016/j.jddst.2015.02.003
- Broadhead, J., Edmond Rouan, S.K., Rhodes, C.T., 1992. The spray drying of pharmaceuticals. *Drug Dev. Ind. Pharm.* 8, 1169–1206. doi:10.3109/03639049209046327
- Cal, K., Sollohub, K., 2010. Spray Drying Technique . I : Hardware and Process Parameters. *J. Pharm. Sci.* 99, 575–586. doi:10.1002/jps
- Casella, R., Williams, D.A., Jambhekar, S.S., 1998. Solid-state β -cyclodextrin complexes containing indomethacin , ammonia and water . I . Formation studies. *Int. J. Pharm.* 165, 1–14. doi:10.1016/S0378-5173(97)00330-X

- Draheim, C., de Crécy, F., Hansen, S., Collnot, E.-M., Lehr, C.-M., 2015. A Design of Experiment Study of Nanoprecipitation and Nano Spray Drying as Processes to Prepare PLGA Nano- and Microparticles with Defined Sizes and Size Distributions. *Pharm. Res.* doi:10.1007/s11095-015-1647-9
- Fahr, A., Liu, X., 2007. Drug delivery strategies for poorly water-soluble drugs. *Expert Opin. Drug Deliv.* 4, 403–16. doi:10.1517/17425247.4.4.403
- Fontana, M.C., Durli, T.L., Pohlmann, A.R., Guterres, S.S., Beck, R.C.R., 2014. Polymeric controlled release inhalable powder produced by vibrational spray-drying: One-step preparation and in vitro lung deposition. *Powder Technol.* 258, 49–59. doi:10.1016/j.powtec.2014.03.011
- Glasmacher, A., Prentice, A., 2006. Current experience with itraconazole in neutropenic patients: a concise overview of pharmacological properties and use in prophylactic and empirical antifungal therapy. *Clin. Microbiol. Infect.* 12, 84–90. doi:10.1111/j.1469-0691.2006.01609.x
- Humberstone, A.J., Charman, W.N., 1997. Lipid-based vehicles for the oral delivery of poorly water soluble drugs. *Adv. Drug Deliv. Rev.* 25, 103–128. doi:10.1016/S0169-409X(96)00494-2
- Ignatious, F., Sun, L., Lee, C.-P., Baldoni, J., 2010. Electrospun nanofibers in oral drug delivery. *Pharm. Res.* 27, 576–88. doi:10.1007/s11095-010-0061-6
- Janssens, S., De Zeure, A., Paudel, A., Van Humbeeck, J., Rombaut, P., Van den Mooter, G., 2010. Influence of preparation methods on solid state supersaturation of amorphous solid dispersions: a case study with itraconazole and eudragit e100. *Pharm. Res.* 27, 775–85. doi:10.1007/s11095-010-0069-y
- Jung, J.Y., Yoo, S.D., Lee, S.H., Kim, K.H., Yoon, D.S., Lee, K.H., 1999. Enhanced solubility and dissolution rate of itraconazole by a solid dispersion technique. *Int. J. Pharm.* 187, 209–18.
- Kawabata, Y., Wada, K., Nakatani, M., Yamada, S., Onoue, S., 2011. Formulation design for poorly water-soluble drugs based on biopharmaceutics classification system: basic approaches and practical applications. *Int. J. Pharm.* 420, 1–10. doi:10.1016/j.ijpharm.2011.08.032
- Kenawy, E.-R., Bowlin, G.L., Mansfield, K., Layman, J., Simpson, D.G., Sanders, E.H., Wnek, G.E., 2002. Release of tetracycline hydrochloride from electrospun poly(ethylene-co-vinylacetate), poly(lactic acid), and a blend. *J. Control. Release* 81, 57–64. doi:10.1016/S0168-3659(02)00041-X
- Kim, Y.M., Sung, Y. Bin, Jang, R.S., Ahn, K.R., 2003. A manufacturing device and the method of preparing for the nanofibers via electroblowing spinning process. *WO 03/080905 A1*.
- Macarron, R., 2006. Critical review of the role of HTS in drug discovery. *Drug Discov. Today* 11, 277–9. doi:10.1016/j.drudis.2006.02.001

- Nagy, Z.K., Balogh, A., Démuth, B., Pataki, H., Vigh, T., Szabó, B., Molnár, K., Schmidt, B.T., Horák, P., Marosi, G., Verreck, G., Van Assche, I., Brewster, M.E., 2015. High speed electrospinning for scaled-up production of amorphous solid dispersion of itraconazole. *Int. J. Pharm.* 480, 137–42. doi:10.1016/j.ijpharm.2015.01.025
- Nagy, Z.K., Nyúl, K., Wagner, I., Molnár, K., Marosi, G., 2010. Electrospun water soluble polymer mat for ultrafast release of Donepezil HCl. *eXPRESS Polym. Lett.* 4, 763–772. doi:10.3144/expresspolymlett.2010.92
- Sarode, A.L., Wang, P., Obara, S., Worthen, D.R., 2014. Supersaturation, nucleation, and crystal growth during single- and biphasic dissolution of amorphous solid dispersions: polymer effects and implications for oral bioavailability enhancement of poorly water soluble drugs. *Eur. J. Pharm. Biopharm.* 86, 351–60. doi:10.1016/j.ejpb.2013.10.005
- Sekiguchi, K., Obi, N., Ueda, Y., 1964. Studies on Absorption of Eutectic Mixture. II. Absorption of Fused Conglomerates of Chloramphenicol and Urea in Rabbits. *Chem. Pharm. Bull* 12, 134–144.
- Simonelli, A.P., Mehta, S.C., Higuchi, W.I., 1969. Dissolution Rates of High Energy Polyvinylpyrrolidone (PVP) Sulfathiazole Coprecipitates. *Jourirul Pharm. Sci.* 58, 538–549. doi:10.1002/jps.2600580503
- Six, K., Berghmans, H., Leuner, C., Dressman, J., Van Werde, K., Mullens, J., Benoist, L., Thimon, M., Meublât, L., Verreck, G., Peeters, J., Brewster, M., Van den Mooter, G., 2003. Characterization of solid dispersions of itraconazole and hydroxypropylmethylcellulose prepared by melt extrusion, Part II. *Pharm. Res.* 20, 1047–54.
- Six, K., Leuner, C., Dressman, J., Verreck, G., Peeters, J., Blaton, N., Augustijns, P., Kinget, R., Van den Mooter, G., 2002. Thermal Properties of Hot-Stage Extrudates of Itraconazole and Eudragit E100. Phase separation and polymorphism. *J. Therm. Anal. Calorim.* 68, 591–601. doi:10.1023/A:1016056222881
- Sóti, P.L., Nagy, Z.K., Serneels, G., Vajna, B., Farkas, A., Van der Gucht, F., Fekete, P., Vigh, T., Wagner, I., Balogh, A., Pataki, H., Mező, G., Marosi, G., 2015. Preparation and comparison of spray dried and electrospun bioresorbable drug delivery systems. *Eur. Polym. J.* doi:10.1016/j.eurpolymj.2015.03.035
- Torchilin, V.P., 2007. Micellar nanocarriers: pharmaceutical perspectives. *Pharm. Res.* 24, 1–16. doi:10.1007/s11095-006-9132-0
- Van Drooge, D.J., Hinrichs, W.L.J., Visser, M.R., Frijlink, H.W., 2006. Characterization of the molecular distribution of drugs in glassy solid dispersions at the nano-meter scale, using differential scanning calorimetry and gravimetric water vapour sorption techniques. *Int. J. Pharm.* 310, 220–229. doi:10.1016/j.ijpharm.2005.12.007
- Vasconcelos, T., Sarmiento, B., Costa, P., 2007. Solid dispersions as strategy to improve oral bioavailability of poor water soluble drugs. *Drug Discov. Today* 12, 1068–75. doi:10.1016/j.drudis.2007.09.005

- Vigh, T., Horváthová, T., Balogh, A., Sóti, P.L., Drávavölgyi, G., Nagy, Z.K., Marosi, G., 2013. Polymer-free and polyvinylpyrrolidone-based electrospun solid dosage forms for drug dissolution enhancement. *Eur. J. Pharm. Sci.* 49, 595–602. doi:10.1016/j.ejps.2013.04.034
- Whitney, W.R., Noyes, A.A., 1897. The rate of solution of solide substances in thier own solutions. *J. Am. Chem. Soc.* 19 (12), 930–934. doi:10.1021/ja02086a003
- Wong, S.M., Kellaway, I.W., Murdan, S., 2006. Enhancement of the dissolution rate and oral absorption of a poorly water soluble drug by formation of surfactant-containing microparticles. *Int. J. Pharm.* 317, 61–8. doi:10.1016/j.ijpharm.2006.03.001
- Wu, C.-Y., Benet, L.Z., 2005. Predicting Drug Disposition via Application of BCS: Transport/Absorption/ Elimination Interplay and Development of a Biopharmaceutics Drug Disposition Classification System. *Pharm. Res.* 22, 11–23. doi:10.1007/s11095-004-9004-4
- Yu, D.-G., Wang, X., Li, X.Y., Chian, W., Li, Y., Liao, Y.Z., 2013. Electrospun biphasic drug release polyvinylpyrrolidone/ethyl cellulose core/sheath nanofibers. *Acta Biomater.* 9, 5665–72. doi:10.1016/j.actbio.2012.10.021
- Yu, D.-G., Yang, J.-M., Branford-White, C., Lu, P., Zhang, L., Zhu, L.-M., 2010. Third generation solid dispersions of ferulic acid in electrospun composite nanofibers. *Int. J. Pharm.* 400, 158–64. doi:10.1016/j.ijpharm.2010.08.010
- Yu, D.-G., Zhu, L.-M., Branford-White, C.J., Yang, J.-H., Wang, X., Li, Y., Qian, W., 2011. Solid dispersions in the form of electrospun core-sheath nanofibers. *Int. J. Nanomedicine* 6, 3271–3280. doi:10.2147/IJN.S27468
- Zhou, F.-L., Gong, R.-H., Porat, I., 2009. Mass production of nanofibre assemblies by electrostatic spinning. *Polym. Int.* 58, 331–342. doi:10.1002/pi.2521

Figure captions

Figure 1 SEM images of samples: ES_20 (a); ES_40 (b); EB_20 (c); EB_40 (d); SD_20 (e) and SD_40 (f); scale bar: 10 μm

Figure 2 X-ray powder diffractions pattern of solid dispersions **A**: ES_20 0 day (a); ES_20 90 days (b); EB_20 0 day (c); EB_20 90 days (d); SD_20 0 day (e); SD_20 90 days (f); physical mixture of 20 w/w% ITR and polymer (g); **B**: ES_40 0 day (a); ES_40 90 days (b); EB_40 0 day (c); EB_40 90 days (d); SD_40 0 day (e) and SD_40 90 days (f)

Figure 3 Measured DSC curves of Eudragit E (a), crystalline ITR (b), and SD_40 (c)

Figure 4 DSC curves of ES_20 (a); EB_20 (b); SD_20 (c) directly after production, and of the physical mixture of 20% w/w ITR and polymer (d). The arrows indicate the ITR melting endotherms.

Figure 5 Raman maps of solid dispersions directly after production: ES_20 (a); EB_20 (b); SD_20 (c); ES_40 (d); EB_40 (e) and SD_40 (f). The arrows indicate the inhomogeneity of ITR distribution (the scales indicate the spectral concentrations of amorphous ITR).

Figure 6 Dissolution profiles of solid dispersions directly after the production (0) and following a three-month storage (90). The error bars indicate \pm S.D. (n = 3).

Figure 7 Wettability of EB samples containing 20% w/w (a) and 40% w/w (b) ITR (repeated measurement; n = 3)

Table 1 Applied technologies and parameters

Technology parameters	Technologies		
	ES	EB	SD
Polymer concentration (wt%)	12	17	2.4
Solution feeding rate (mL/g)	10	200	150
Nozzle-to-collector distance (m)	0.25	0.30	-
Applied voltage (kV)	30	50	-
Nozzle internal diameter (mm)	0.75	0.75	0.4
Spray air pressure (bar)	-	1	0.5
Drying air flow rate (m ³ /min)	-	-	0.3
Drying air temperature (°C)	25	25	70
Cooling air flow rate (m ³ /min)	-	-	0.27

Table 2 Yields, composition, and content uniformity of ITR loaded solid dispersions prepared by various technologies

Sample code	Technology	Nominal concentration of ITR in the solid dispersions (w/w%)	Yields ^a (%)	Productivity (g/h)	ITR content in solid dispersions (%) ^b
Cryst. ITR	-	100	-	-	99.8 ± 0.5
ES_20	ES	20	71	1.5	100.2 ± 0.7
ES_40	ES	40	73	2	100.8 ± 0.6
EB_20	EB	20	62	42.5	100.5 ± 0.9
EB_40	EB	40	66	56.7	100.4 ± 0.4
SD_20	SD	20	51	4.5	100.0 ± 0.7
SD_40	SD	40	65	9	100.7 ± 0.8

^a The yields were determined based on outcome of the solid product related to the solid starting materials. ^b Mean ± S.D. for three repeated measurement.

Table 3 The concentration of residual solvents in solid dispersions

Sample	c (µg/g, ppm) methanol	c (µg/g, ppm) dichloromethane
LLOQ ^a	1000	15
Cryst. ITR	<1000	<15
ES_20	<1000	<15
ES_40	<1000	<15
EB_20	<1000	<15
EB_40	<1000	<15
SD_20	<1000	<15
SD_40	<1000	21
LRS ^b	3000	600

^a LLOQ: lower limit of quantification, ^b LRS: limit of residual solvent (Guideline for Residual Solvents, European Medicines Agency 2010)

Table 4 Initial crystallinity of ITR in the polymer matrix (90 indicates the storage days)

note: $\Delta H_{110-175}$ means the sum of heat induced crystallization and melting peaks of ITR in the samples (<3% means that the difference of the two values is below the detection level).

*Related to the ITR content of samples.

Entry	Mesophase transition		Calculated initial crystallinity of ITR	
	Temperature (°C)	ΔH_{Mt} (J/g)	$\Delta H_{110-175}$ (J/g)	w/w%*
Cryst. ITR	-	-	94.05	100
ES_20	-	<0.06	<0.94	<3
EB_20	-	<0.06	<0.94	<3
SD_20	87.40	0.07	<0.94	<3
ES_40	89.03	0.27	<0.94	<3
EB_40	88.95	0.25	<0.94	<3
SD_40	89.45	0.36	<0.94	<3
ES_20_90	-	<0.06	<0.94	<3
EB_20_90	-	<0.06	<0.94	<3
SD_20_90	88.43	0.06	1.69	9
ES_40_90	89.12	0.36	<0.94	<3
EB_40_90	89.38	0.16	<0.94	<3
SD_40_90	89.54	0.37	3.86	10

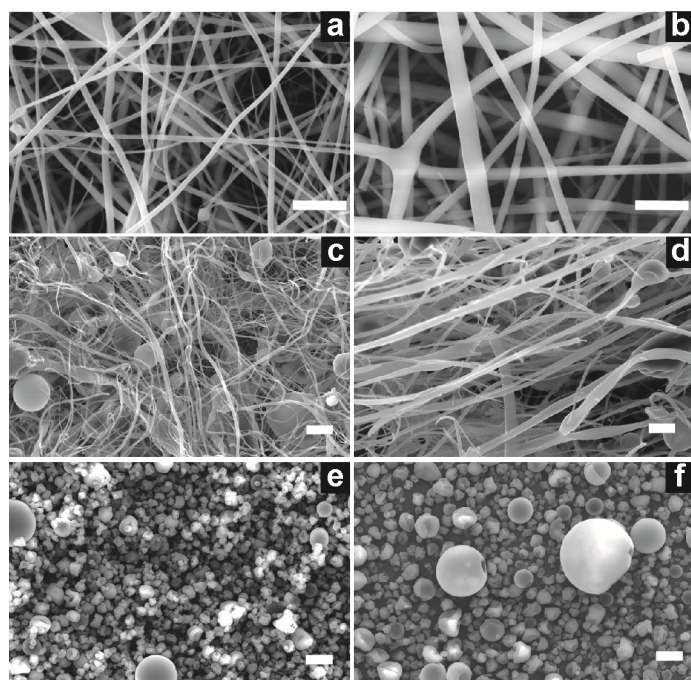


Fig. 1

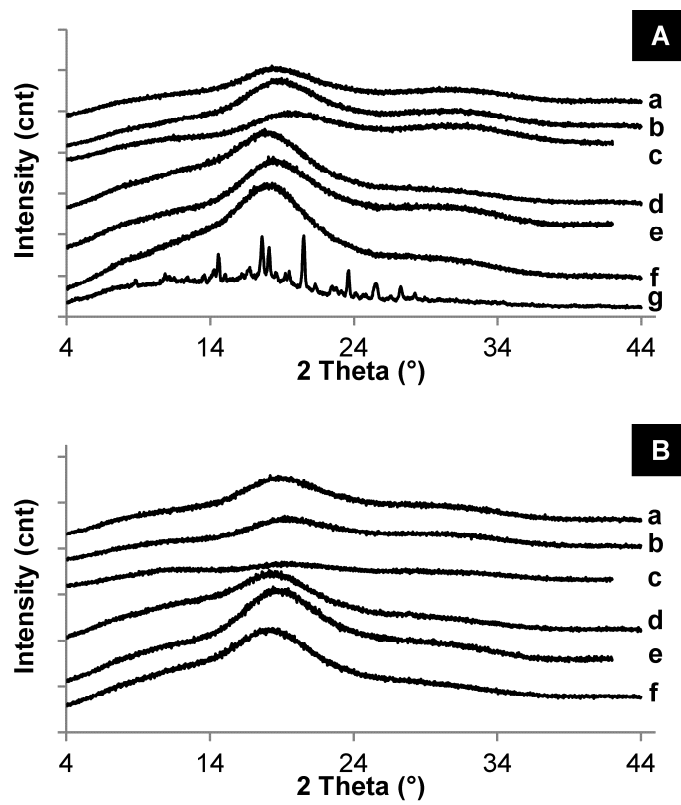


Fig. 2

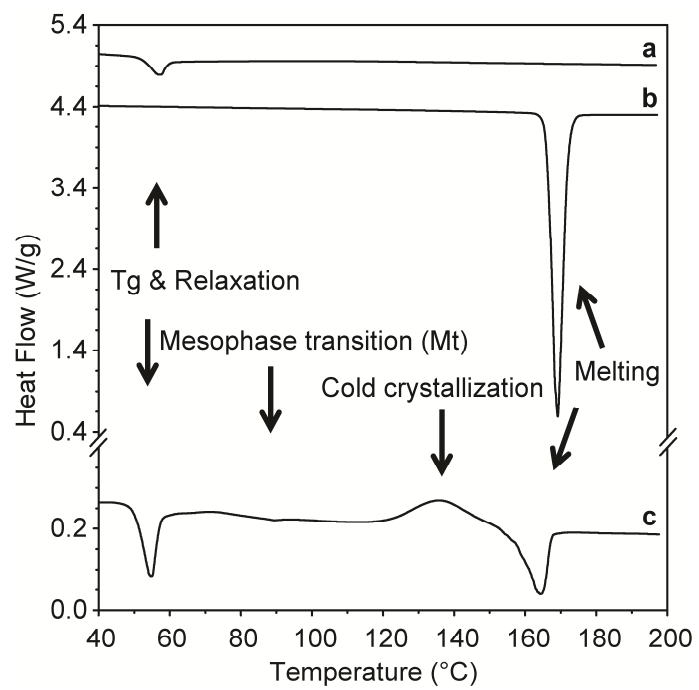


Fig. 3

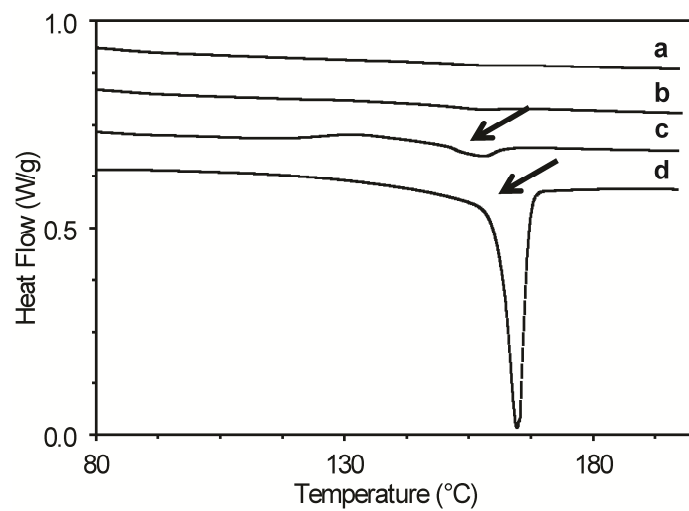


Fig. 4

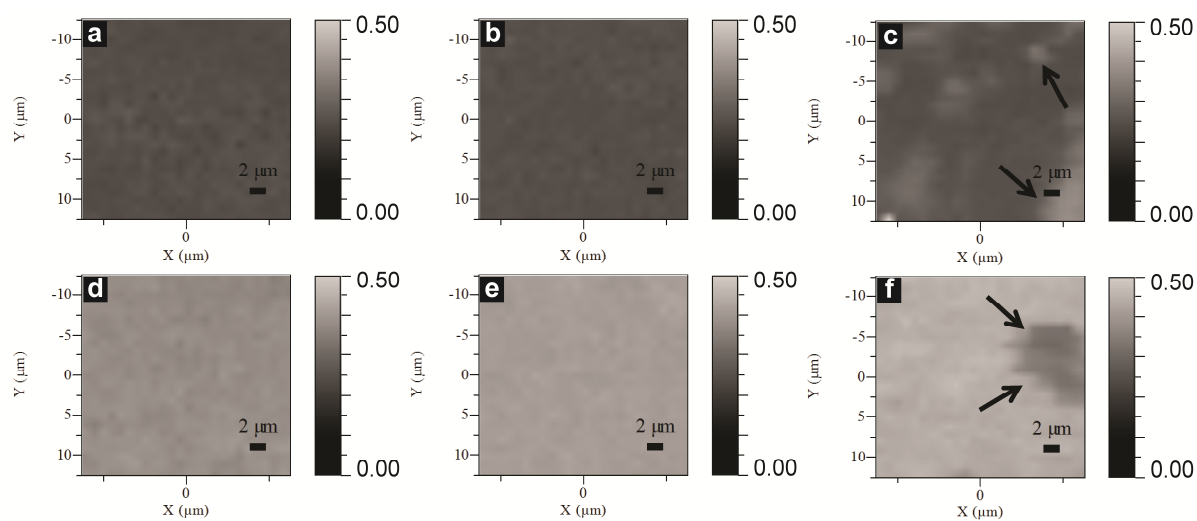


Fig. 5

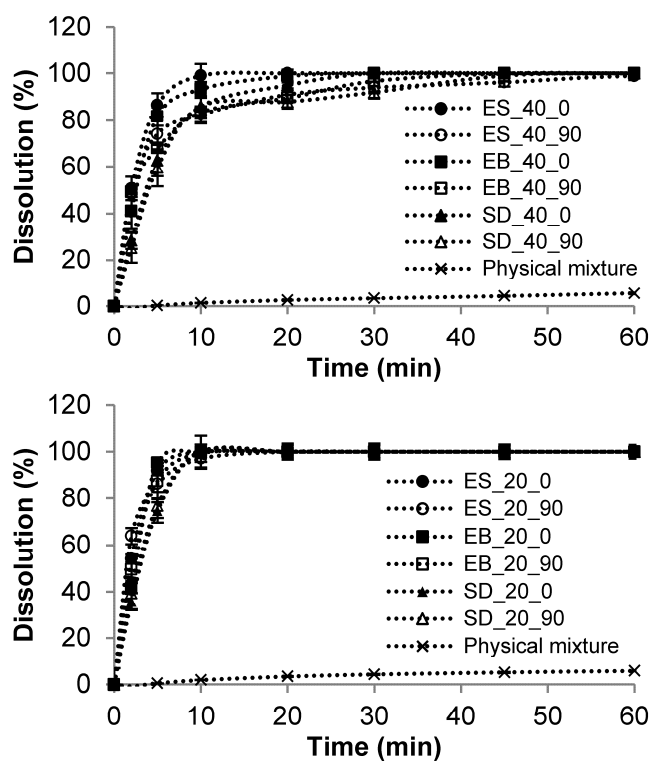


Fig. 6

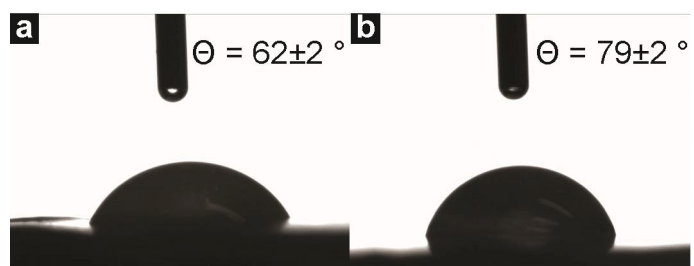


Fig. 7